Short communication

Escalating CO_2 degassing at the Pisciarelli fumarolic system, and implications for the ongoing Campi Flegrei unrest

G. Tamburello *, S. Caliro , G. Chiodini , P. De Martino , R. Avino , C. Minopoli , A. Carandente , D. Rouwet , A. Aiuppa , A. Costa , M. Bitetto , G. Giudice , V. Francofonte , T. Ricci , A. Sciarra , E. Bagnato , F. Capecchiacci

Istituto Nazionale di Geofisica e Vulcanologia, Sezione di Bologna, via Donato Creti, 12, 40128 Bologna, Italy

ARTICLE INFO

ABSTRACT

This short communication aims at providing an updated report on degassing activity and ground deformation variations observed during the ongoing (2012–2019) Campi Flegrei caldera unrest, with a particular focus on Pisciarelli, currently its most active fumarolic field. We show that the CO_2 flux from the main Pisciarelli fumarolic vent (referred as "Soffione") has increased by a factor >3 since 2012, reaching in 2018–2019 levels (>600 tons/day) that are comparable to those typical of a medium-sized erupting arc volcano. A substantial widening of the degassing vents and bubbling pools, and a further increase in CO_2 concentrations in ambient air (up to 6000 ppm), have also been detected since mid-2018. We interpret this escalating CO_2 degassing activity using a multidisciplinary dataset that includes thermodynamically estimated pressures for the source hydrothermal system, seismic and ground deformation data. From this analysis, we show that degassing, deformation and seismicity have all reached in 2018–2019 levels never observed since the onset of the unrest in 2005, with an overall uplift of ~57 cm and ~448 seismic events in the last year. The calculated pressure of the Campi Flegrei hydrothermal system has reached ~44 bar and is rapidly increasing. Our results raise concern on the possible evolution of the Campi Flegrei unrest and reinforce the need for careful monitoring of the degassing activity at Pisciarelli, hopefully with the deployment of additional permanent gas monitoring units.

© 2019.

1. Introduction

The Campi Flegrei caldera (CFc) near Naples (Italy), one of the most densely populated volcanic areas in the world, has shown signs of unrest since the 1950s–1980s, during which three major cycles of uplift/subsidence and seismic swarms (both united in the term "bradyseisms") occurred (Barberi et al., 1984; Del Gaudio et al., 2010). A new uplift phase started in November 2005 (De Martino et al., 2014), accompanied by increased seismicity and degassing activity, and compositional changes in the emitted fluids (Chiodini et al., 2012, 2016). Hydrothermal-volcanic fluid release is today centered around the Solfatara, a ~3.8 kyr old tuff cone in the center of the Caldera (Isaia et al., 2009; Fig. 1), and takes the form of both widespread soil diffuse degassing (Cardellini et al., 2017) and intense fumarolic vent discharge (Chiodini et al., 2012). The strongest fumarolic emissions are located at Solfatara and, approximately 400 m eastward, at Pisciarelli (Fig. 1). The fumarolic field of Pisciarelli (a 0.03 km² fault-related hydrothermal area), in particular, has been the locus of recent shallow seismicity recorded by the seismic network of the local volcanic observatory (Istituto Nazionale di Geofisica e Vulcanologia, Osservatorio Vesuviano, INGV-OV, http://www.ov.ingv.it/

ov/) and has shown clear signs of increasing hydrothermal activity during the ongoing phase of unrest. Pisciarelli is today characterized by the presence of large mud pools (water temperature ~90 °C) with intense bubbling, and by high flow rate fumaroles emitting a H_2O-CO_2 rich gas mixture with minor H_2S. The majority of the gas is emitted from a vent (gas temperature ~114 °C) that opened in 2009 and that, since then, visibly increased its degassing activity (Chiodini et al., 2015). One particularly vigorous fumarole, from here on simply referred as Soffione fumarole, radiates seismic tremor which RSAM (real-time seismic-amplitude measurement) increased by at least one order of magnitude in the 2010–2016 period (Chiodini et al., 2017a, 2017b).

Previous work has demonstrated that hydrothermal activity at Pisciarelli today produces several kilotons of vapor and gas every day (Aiuppa et al., 2013, 2015; Queißer et al., 2017). The 20 years-long fluid-related thermal energy output from CFc is $\sim 5 \cdot 10^{16}$ J (Chiodini et al., 2017a, 2017b), corresponding to an average heat flux of ~80 MW. This volatile-heat output is supplied by volatiles from the underlying magmatic/hydrothermal system, and, given the surrounding densely populated area, raises concerns on the possible development of thermal and/or mechanical instabilities in the subsurface of CFc, in particular of Pisciarelli, that can ultimately trigger phreatic activity (Isaia et al., 2015; Mayer et al., 2016). Ultimately, this escalating transport of deeply derived CO_2 also raises the question of the extent to which
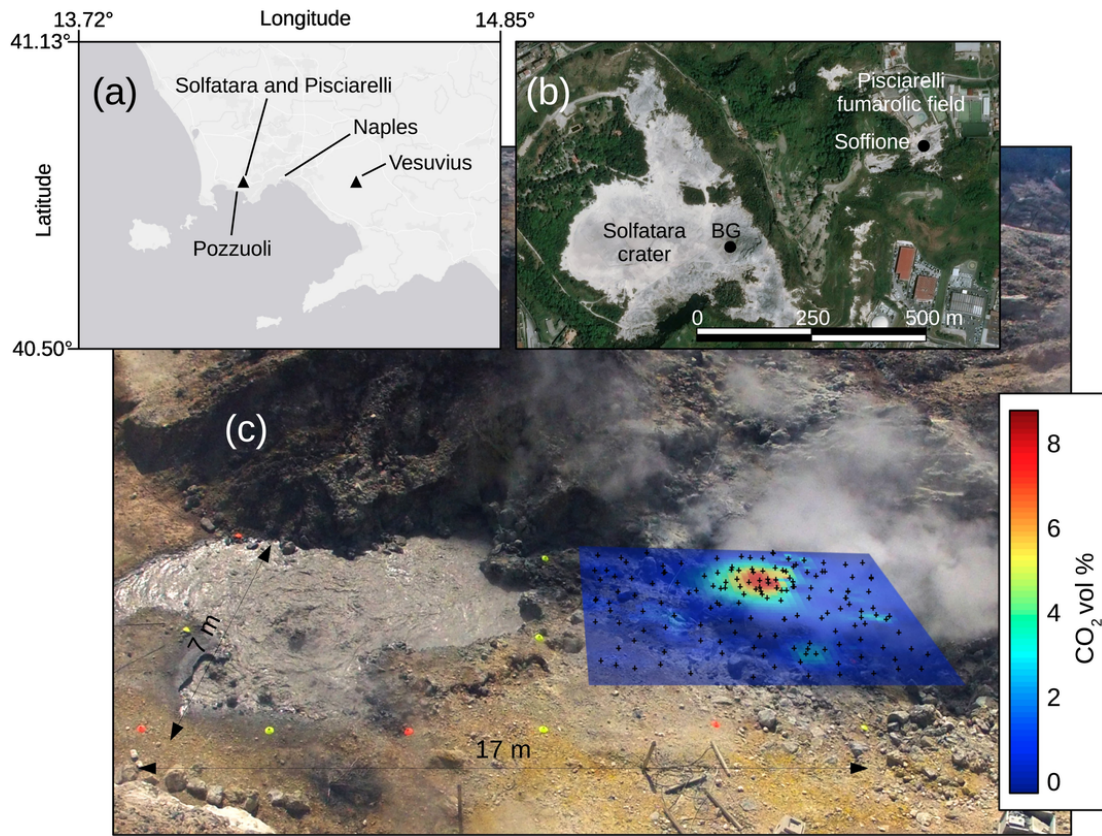
Fig. 1. (a) Sketch map of the Naples metropolitan area in Central Italy and the position of the active volcanic systems. (b) Satellite picture of Solfatara crater and Pisciarelli fumarolic field and the position of their two main fumaroles discussed in this work. © Photo of the bubbling pool and fumaroles of Pisciarelli on 28th July 2017. The yellow and orange cones make a grid of 17×7 m. The MG measurements, carried out for ~1 h above the Soffione, are localized manually and the pixel coordinates (black crosses) are converted in metric coordinates referred to the local grid. The pseudo colors show the high concentrations of CO_2 at 1 m height above the fumarole. (For interpretation of the references to colour in this figure legend, the reader is referred to the web version of this article.)

magma ascent and storage is implicated (Chiodini et al., 2016; D'Auria et al., 2016).

Here, we provide novel information on the ongoing degassing activity at CFc by presenting new CO_2 and H_2S gas flux measurements recorded since 2012 at the Soffione fumarole. We integrate the existing data set with results of new surveys, performed since 2014, using an ad-hoc method that combines video footages and gas measurements to obtaining high-precision concentration maps of gas emissions. Our gas flux data, combined with model results (thermodynamically derived pressure and temperature conditions of the hydrothermal system), reveal escalating degassing activity at Pisciarelli and raise concerns on the possible future evolution of the volcanic system.

2. Method

The new gas flux data presented here were obtained during periodic gas surveys conducted with a multi-component gas analyzer system (MultiGAS). We employed the same measurement setup used previously (Aiuppa et al., 2013; Bagnato et al., 2013), but with an improved georeferencing method, as described below (Fig. 1).

During each campaign, measurements were filmed by a GoPro camera placed on a spur of rock ~10 m above the Soffione fumarole and capturing an image of the degassing area every 2 s. A regular grid was built in the field with colored (yellow and orange) marker cones spaced every 1–2 m in order to encircle the measured vent (Fig. 1). Each cone was easily localized in the photos and represented by X_p-Y_p pixel coordinates. This procedure allowed fitting the points in a X_p-Y_p-X_m and X_p-Y_p-Y_m space with a second degree polynomial surface (with the subscript m indicating the X-Y coordinates, in meters, of each cone referred to a local reference system; usually the origin is set at the bottom left cone in the photos) and using the obtained equation to convert pixel coordinates into local metric coordinates.

Gas concentrations were measured along the measurement grid with a MultiGAS equipped with (i) an infrared sensor for CO_2 (Edinburg Gascard, 0–10% range), (ii) an electrochemical sensor for H_2S (City Technology, 0–200 ppm range), and (iii) a ~1 l/min membrane pump to collect the external gas. Gas concentration measurements were taken every 2 s. The MultiGAS was connected to a 5 m long silicon tube (2 mm internal diameter) sustained by a rigid probe and measuring the gas concentrations at a constant elevation from the ground (~1 m). A colored funnel and a hydrophobic PTFE filter (1.0 μm filter pore size, 50 mm diameter) were attached to the gas inlet to prevent liquid water from entering the MultiGAS, and to make it more visible for being localized in the photos. Each measurement, held in each location for 10–20 s approximately, was georeferenced by manually picking the position of the gas inlet in each image and converting pixels in meters using the retrieved polynomial equation described above. The gas inlet tracking was performed with the software ImageJ and the MTrackJ plug-in (Abramoff et al., 2004). This operation allowed reducing the error of the gas inlet position approximately to few centimeters. Hence, the retrieved georeferenced CO_2 and H_2S concentrations were interpolated along a surface roughly orthogonal to the vertical plume transport speed, approximated using a

multilevel B-splines (Lee et al., 1997), and subsequently 2D-integrated to obtain the integrated column amounts (ICAs, in kg·m^{-1}) for each gas. Ultimately, gas fluxes were calculated by multiplying ICAs by the vertical plume transport speeds (in m·s^{-1}). The latter were obtained by manually tracking the rising gas fronts using MTrackJ to process close-up videos (at 25 fps) of the fumarole filmed with a Go-Pro (Aiuppa et al., 2013, 2015).

In principle, both CO_2 and H_2S gas fluxes can be calculated following the above procedure and starting from the concentrations map of each gas separately. However, the CO_2 (infrared) and H_2S (electrochemical) sensors have diverse response times, with the former being typically a few seconds faster (T90 < 10 s and <35 s respectively). Thus, because the slower response times of the H_2S sensor that may have led to errors into individual H_2S determinations, the H_2S fluxes were only calculated indirectly from the CO_2 flux by using the relation $H_2S_{flux} = CO_{2,flux} \cdot (CO_2/H_2S)_{weight}$ (where the latter is the time-averaged mean CO_2/H_2S ratio of the Soffione fumarole, obtained from the slope of the best-fit regression line in a CO_2 vs H_2S scatter plot drawn for the entire dataset).

The acquired images of the fumarolic field of Pisciarelli also allowed us to follow the temporal evolution of the geometry of the main bubbling pool of Pisciarelli. We tracked the perimeter of the pool using ImageJ software, converted pixels into meters and calculated its area for 8 campaigns since 2012.

Our gas flux results were complemented by an updated dataset of the equilibrium pressures of the hydrothermal reservoir, estimated by solving H_2O-H_2-CO_2-CO gas equilibria (sensitive to T-P conditions) from the measured compositions of Solfatara fumaroles. The thermodynamic calculations are the same as those reported in Chiodini et al. (2017a, 2017b) and are based on gas equilibria within the H_2O-CO_2-H_2-CO gas system applied to the highest temperature fumarole of Solfatara (BG fumarole, T ~160 °C). The BG fumarole is sampled monthly by the INGV-OV and previous work demonstrated that the fumarole discharge fluids are suitable for the application of gas geothermometric and geobarometric techniques (e.g. Caliro et al., 2007 and references therein; Chiodini et al., 2015). A different approach to hydrothermal gas equilibria of Solfatara system was proposed by Moretti et al. (2017) and is widely debated in Chiodini et al. (2017a, 2017b) and Cardellini et al. (2017). On the contrary, the fumaroles of Pisciarelli are sampled more sporadically and are affected by shallow secondary processes (Chiodini et al., 2011). In particular, their CO/CO_2 ratio (and, consequently, the P-T estimations that derive from them) exhibits marked seasonal cycles (see for example Figs. 7 and 8 in Chiodini et al., 2011), which are interpreted as reflecting variable interactions with meteoric water during dry and wet seasons. The BG time-series suffered from a data gap between September 2017 and January 2018, when sampling was precluded by the closing of the access to Solfatara crater after the tragic fatalities by asphyxiation of 3 people inside a pit-hole (https://www.bbc.com/news/world-europe-41243134). Gas sampling regularly restarted in February 2019.

We additionally presented updated records of daily CO_2 ambient air concentrations (with the exception of 10 data gaps longer than 1 week due to technical problems) measured at 40 cm from the ground by an automatic station located in the surroundings of the fumarolic area (~20 m SE from Soffione fumarole) that has been shown to be a good proxy for the total volcanic gas release (for more details, see Chiodini et al., 2017a, 2017b).

A continuous GPS (cGPS) network of 25 stations is currently operating at CFc (De Martino et al., 2014; Iannaccone et al., 2018). In this work, we only considered data from the RITE cGPS station, located at Pozzuoli (Fig. 1a) in the area of maximum vertical displacement. This station is commonly adopted as representative of the vertical deformation history at the CFc.

Finally, we followed the same procedure described in Chiodini et al. (2017a, 2017b) to extract the CFc background seismicity from the seismic catalogue. We report seismicity as the cumulative number of seismic events with inter-arrival times higher than 1 day.

3. Results and discussion

Fig. 2a–b illustrates the temporal evolution of CO_2 ICAs and fluxes for the Soffione fumarole. The CO_2 ICA time-series, by itself a good proxy for the degassing process occurring at Pisciarelli, highlights a factor ~3 ICA increase since 2012 (Fig. 2a). Such an increase is also evident considering the CO_2 fluxes, derived by combining the ICAs with the vertical plume speed (Fig. 2b).

Our CO_2 gas flux results are consistent with those independently measured (by a combination of laser spectroscopy remote-sensing techniques) in the period 2012–2017 (Pedone et al., 2014; Aiuppa et al., 2015; Queißer et al., 2017). The latter laser-based observations correspond to the total gas contributions from the Pisciarelli area, e.g., they include the gas output from Soffione and from the many mud pools and small fumaroles nearby.

The recorded H_2S ICAs and fluxes (Fig. 2c), calculated from the CO_2 fluxes as explained in the Method section, exhibit low values but still maintain an increasing trend (in light of the constant CO_2/H_2S weight ratio of 360±90 measured at Soffione). This relatively modest sulfur transport and release at Pisciarelli is corroborated by ~~our~~ previous SO_2 observations (Aiuppa et al., 2013). Until now, SO_2 in the fumarolic gases sampled at ~1 m above the ground has remained either absent or at ~0.1 ppm levels at most. We cannot ruled out the possibility that such extremely low SO_2 concentrations are due to secondary effects, such as in-plume H_2S oxidation (Venturi et al., 2019), or merely an artifacts due to cross-interference of H_2S on the SO_2 sensor (the very high H_2S concentrations in the plume could result into <100% effectiveness of H_2S scavenging by the scrubbing filter in front of the SO_2 sensor). We thus cannot further speculate on these SO_2 detections. However, this feature certainly confirms the strong hydrothermal control on sulfur outgassing of CFc, but the high sensitivity of the MultiGAS for detecting low SO_2 concentrations makes it a robust monitoring technique of a possible hydrothermal to magmatic transition in the future.

The escalating CO_2 degassing activity is further supported by ambient air CO_2 concentration records (Fig. 2d). Within the geochemical dataset here presented, the air CO_2 time series, recorded at the permanent soil flux station of Pisciarelli, is characterized by the highest temporal resolution. Our temporal record (Fig. 2d) demonstrates that the daily averaged air CO_2 concentrations increase markedly (by a factor of ~6), from ~1000 ppm in 2012, up to ~6000 ppm in January 2019. Within this trend, the most drastic increase occurred since August 2018, with the air CO_2 rising from ~3000 ppm to ~6000 ppm in only 6 months. We also identify shorter-period variations, perhaps caused by meteorological factors, which we do not aim to remove since we focus on long-period trends. In order to identify the multiple long-period trends characterizing the air CO_2 time series of Pisciarelli, we applied the break detection algorithm described by Verbesselt et al. (2010a, 2010b) using the package "bfast" for the R programming language (R Core Team, 2013). The algorithm breaks the time series into trend components and outputs the occurring times of the breakpoints with a 95% confidence interval and the fitted trend components between the breakpoints (Fig. 2d). We identify 3 important trend changes since 2012, occurred in October 2013, March 2015
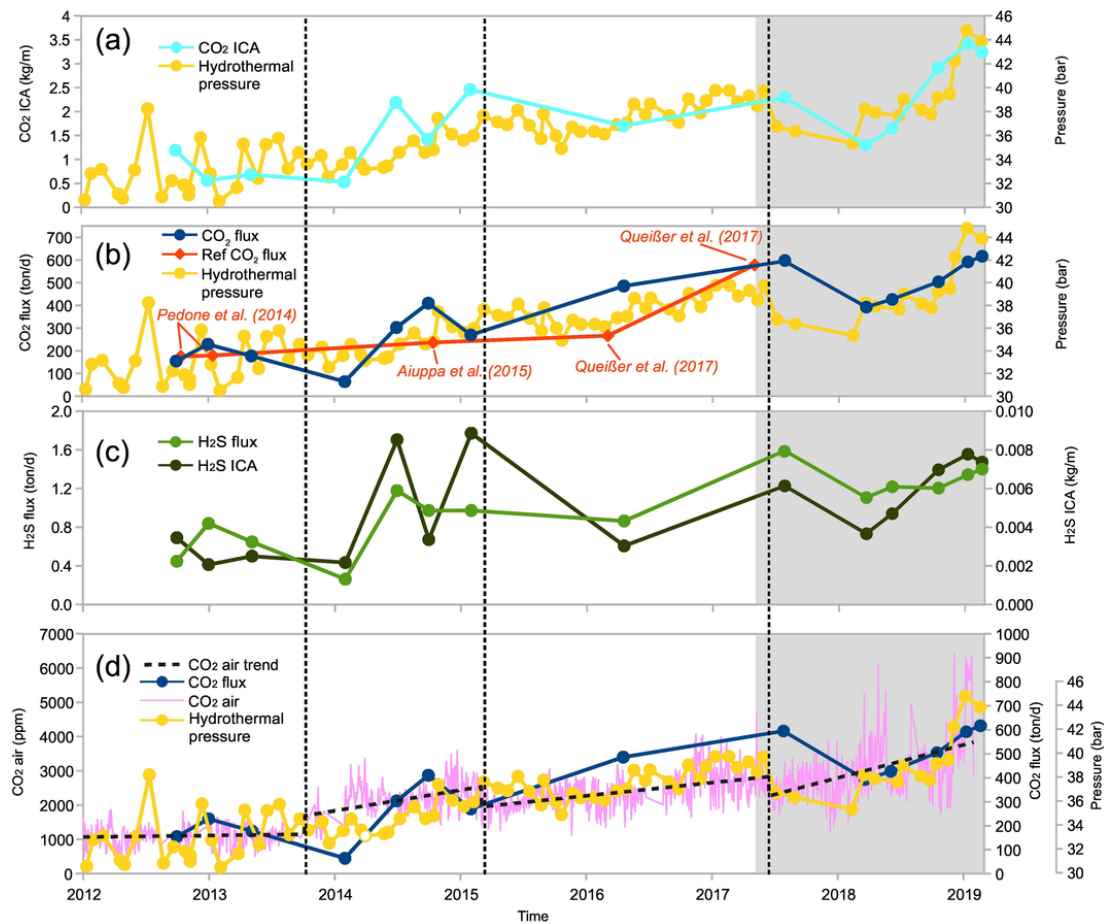
Fig. 2. CO_2 ICA (cyan) and flux (blue) time series of Soffione fumarole are compared to the previous CO_2 flux estimations (red), H_2S ICA (dark green) and flux (green), daily air CO_2 concentrations (magenta) and calculated monthly pressure of the hydrothermal system (yellow). The shadow gray areas show the updated air CO_2 and hydrothermal pressure values. Vertical dashed lines correspond to the breakpoints identified by the "bfast" algorithm and separating 3 trend changes in the air CO_2 time series. (For interpretation of the references to colour in this figure legend, the reader is referred to the web version of this article.)

and June 2017. These break events are evident in almost every time series we reported in this work (Figs. 2–3).

Fig. 2 also compares the data discussed above with the estimated equilibrium pressures of the hydrothermal system, as inferred from La Solfatara fumarole composition (Chiodini et al., 2017a, 2017b). Since 2012, the hydrothermal pressure increased with a constant trend (~1.4 bar/yr, with no breakpoints identified by the bfast algorithm) that stopped on June 2017, when the pressure dropped and then started again to rise at a faster rate (~7 bar/yr). This waning and waxing event is noticeable also in the CO_2 flux time series and identified as breakpoint with the bfast algorithm applied at the air CO_2 time series.

Fig. 3 compares the recorded time-series for geophysical observables with the calculated hydrothermal pressure. All the parameters correlate well and display the same increasing trend. The three breakpoints identified from the air CO_2 time series of Pisciarelli clearly match three plateaux of the background seismicity and ground deformation, which mark a temporary stop in activity escalation. The most recent (June 2017) of these breakpoints in particular, apart from marking a temporary "stasis" of uplift and background seismicity (Fig. 3), is consistently followed by a temporarily decrease of gas flux and hydrothermal pressure, lasting until early 2018 (Fig. 2). The June 2017 "stasis" event is a very short-lived one, however, and is followed by a new activity escalation, the most recent in our dataset.

This manifests into continuous uplift (at 8.5 cm/yr rate, as indicated by the vertical displacement at RITE cGPS station; Fig. 3b), increasing background seismicity (Fig. 3a), shallowing of the seismic activity underneath Pisciarelli (an average of ~1 km in 2019, Figs. 3c and 4), and accelerating degassing (since mid-2018; see the increasing CO_2 fluxes and hydrothermal pressures; Figs. 2 and 3a). This most recent high degassing level is also associated with a visible change in the geometry of the fumarolic field. We observe, in particular, an evident widening of the degassing vents and of the main bubbling pool of Pisciarelli. In order to quantitatively exploring this process, we calculate the area of the bubbling pool from the photographic time series captured by the GoPro since 2012. The area shows nearly constant values (~40 m^2) until mid-2018, posteriorly followed by a rapid increase (Fig. 3d). In fact, the bubbling pool recently widened and more bursting bubbles took place within originating from more vents (Fig. 3e–f).

4. Conclusions

The CFc bradyseisms since 1950 are thought to represent episodes of a single, general unrest that is weakening the underlying crust through processes of stress accumulation, fluid saturation, and heating and pressurization of the hydrothermal reservoir (Di Luccio et al., 2015; Kilburn et al., 2017; Chiodini et al., 2017a, 2017b; Zaccarelli
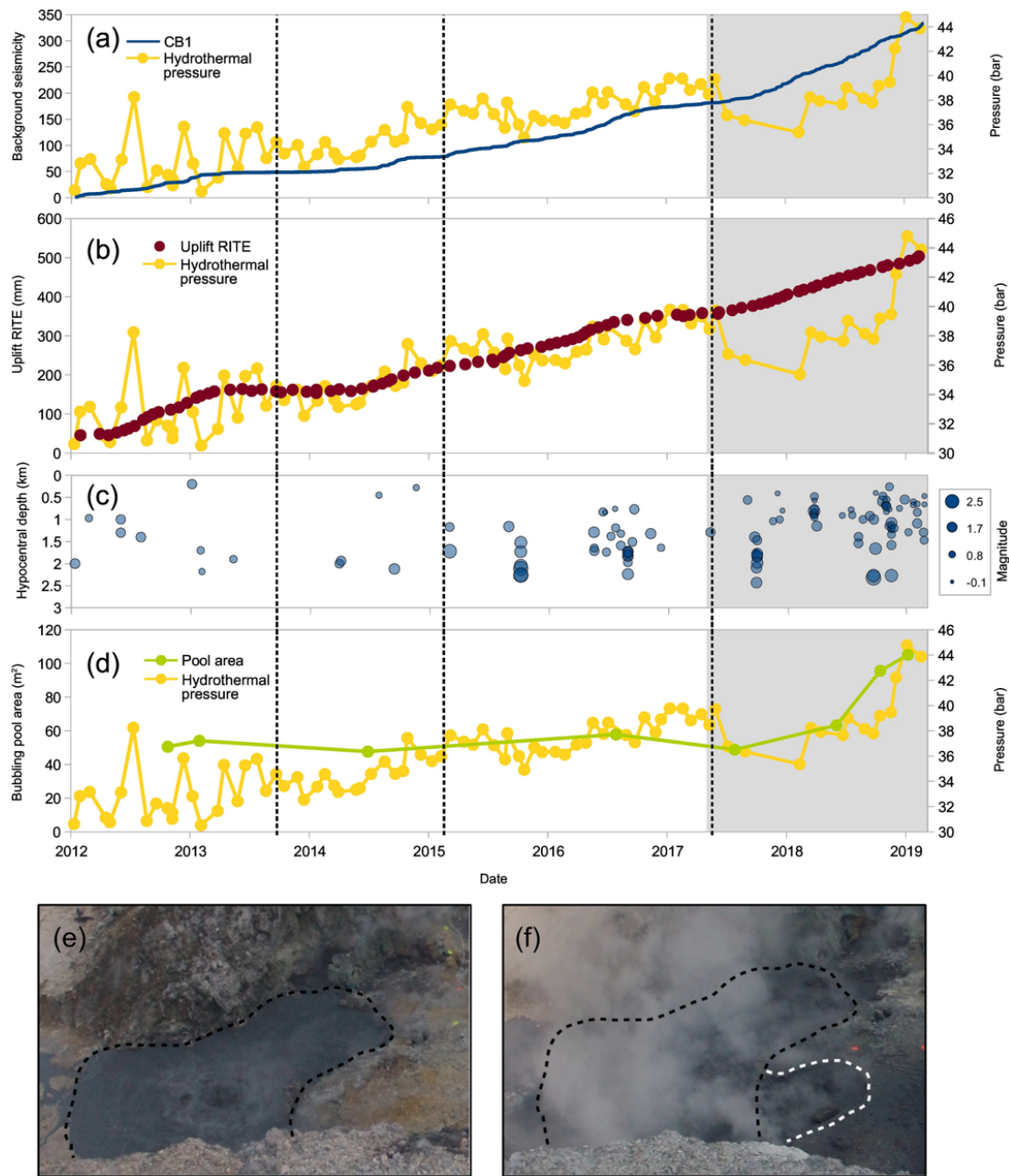
Fig. 3. Geophysical data are compared to the calculated pressure of the hydrothermal system (yellow). (a) Cumulative background seismicity, (b) vertical displacement at RITE cGPS station, (c) hypocentral depth and magnitude of the earthquakes underneath Pisciarelli fumarolic field, (d) area of the main bubbling pool of Pisciarelli and photos of its evolution on (e) October 2018 and (f) February 2019. Vertical dashed lines correspond to the breakpoints identified by the "bfast" algorithm and separating 3 trend changes in the air CO_2 time series shown in Fig. 2. (For interpretation of the references to colour in this figure legend, the reader is referred to the web version of this article.)

and Bianco, 2017). Magmatic intrusions and/or the injection of large amounts of magmatic fluids are thought to have accompanied/triggered these unrests (Amoruso et al., 2014; D'Auria et al., 2015; Chiodini et al., 2016).

Our results identify a clear escalation of degassing activity at Pisciarelli since 2012 and thus raise concern on a possible acceleration of the unrest. Today, the Soffione fumarole releases >600 tons/day of CO_2, equivalent to what daily discharged by a medium-sized arc volcano recently (e.g., Galeras in Colombia) or currently erupting (e.g., Dukono, in Indonesia; Aiuppa et al., 2019). If we convert the Sof-

fione CO_2 flux value in vapor using the average H_2O/CO_2 mass ratio measured by direct sampling (~1.6 in the period 2017–2018, INGV-OV monitoring data and Chiodini et al., 2017a, 2017b) we obtain >960 tons/day of H_2O, equivalent to >29 MW of energy released from only one fumarole (considering the vapor enthalpy at 114 °C, corresponding to ~2.7 J/g). This heightened magmatic gas transport is pressurizing the shallow hydrothermal systems to levels never observed before at CFc in recent times (Fig. 4). Our results, thus, clearly highlight the need for intensifying volcano monitoring in this densely inhabited volcanic area.
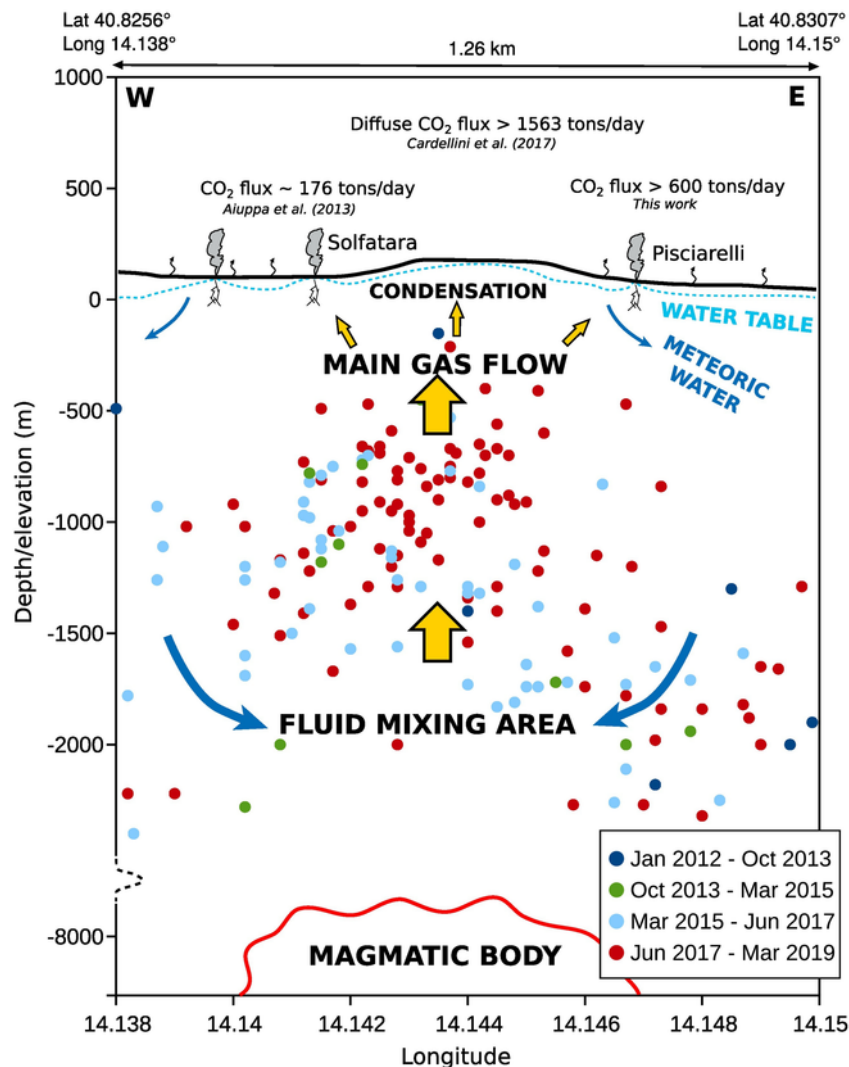
Fig. 4. Conceptual model of the Solfatara-Pisciarelli hydrothermal system (modified after Gresse et al., 2017). This E-W model crosses the main fumarolic areas of Solfatara and Pisciarelli. The hypocentral depth of the earthquakes occurred during 4 periods, separated by the 3 identified break events, are shown.

Acknowledgment

Appendix A. Supplementary data

Supplementary data associated with this article can be found in the online version, at https://doi.org/10.1016/j.jvolgeores.2019.07.005. These data include the Google map of the most important areas described in this article.

References

Abramoff, M.D., Magelhaes, P.J., Ram, S.J., 2004. Image processing with ImageJ. Biophoton. Int. 11, 36–42.

Aiuppa, A., Tamburello, G., Di Napoli, R., Cardellini, C., Chiodini, G., Giudice, G., Grassa, F., Pedone, M., 2013. First observations of the fumarolic gas output from a restless caldera: implications for the current period of unrest (2005–2013) at Campi Flegrei. Geochem. Geophys. Geosyst. 14 (10), 4153–4169. https://doi.org/10.1002/ggge.20261.

Aiuppa, A., Fiorani, L., Santoro, S., Parracino, S., Nuvoli, M., Chiodini, G., Minopoli, C., Tamburello, G., 2015. New ground-based lidar enables volcanic CO2 flux measurements. Sci. Rep. 5 (May), 13614https://doi.org/10.1038/srep13614.

Aiuppa, A., Fischer, T.P., Plank, T., Bani, P., 2019. CO2 flux emissions from the Earth's most actively degassing volcanoes, 2005–2015. Sci. Rep. 9 (2019), 5442.

Amoruso, A., Crescentini, L., Sabbetta, I., De Martino, P., Obrizzo, F., Tammaro, U., 2014. Clues to the cause of the 2011–2013 Campi Flegrei caldera unrest, Italy, from continuous GPS data. Geophys. Res. Lett. 41, 3081–3088. https://doi.org/10.1002/2014GL059539.

Bagnato, E., Tamburello, G., Aiuppa, A., Sprovieri, M., Vougioukalakis, G.E., Parks, M., 2013. Mercury emissions from soils and fumaroles of Nea Kameni volcanic centre, Santorini (Greece). Geochem. J. 47 (4), 437–450.

Barberi, F., Corrado, G., Innocenti, F., Luongo, G., 1984. Phlegraean fields 1982–1984: brief chronicle of a volcano emergency in a densely populated area. Bull. Volcanol. 47 (2), 175–185.

Cardellini, C., Chiodini, G., Frondini, F., Avino, R., Bagnato, E., Caliro, S., Lelli, M., Rosiello, A., 2017. Monitoring diffuse volcanic degassing during volcanic unrests: the case of Campi Flegrei (Italy). Sci. Rep. 7 (1), 6757. https://doi.org/10.1038/s41598-017-06941-2.

Chiodini, G., Caliro, S., De Martino, P., Avino, R., Ghe- pardi, F., 2012. Early signals of new volcanic unrest at Campi Flegrei caldera? Insights from geochemical data and physical simulations. Geology 40, 943–946.

Chiodini, G., Paonita, A., Aiuppa, A., Costa, A., Caliro, S., De Martino, P., Acocella, V., Vandemeulebrouck, J., 2016. Magmas near the critical degassing pressure drive volcanic unrest towards a critical state. Nat. Commun. 7, 1–9. https://doi.org/10.1038/ncomms13712.

Chiodini, G., Giudicepietro, F., Vandemeulebrouck, J., Aiuppa, A., Caliro, S., Cesare, W. De, Tamburello, G., Avino, R., Orazi, M., D'Auria, L., 2017. Fumarolic tremor and geochemical signals during a volcanic unrest. Geology 45 (12), 1131–1134. https://doi.org/10.1130/G39447.1.

Chiodini, G., Selva, J., Del Pezzo, E., Marsan, D., De Siena, L., D'Auria, L., Bianco, F., Caliro, S., De Martino, P., Ricciolino, P., Petrillo, Z., 2017. Clues on the origin of post-2000 earthquakes at Campi Flegrei caldera (Italy). Sci. Rep. 7 (1), 1–10. https://doi.org/10.1038/s41598-017-04845-9.

De Martino, P., Tammaro, U., Obrizzo, F., 2014. GPS time series at Campi Flegrei caldera (2000−2013). Ann. Geophys. 57, S0213.

Gresse, M., Vandemeulebrouck, J., Byrdina, S., Chiodini, G., Revil, A., Johnson, T.C., Metral, L., 2017. Three-dimensional electrical resistivity tomography of the Solfatara Crater (Italy): implication for the multiphase flow structure of the shallow hydrothermal system. J. Geophys. Res. Solid Earth 122 (11), 8749–8768. https://doi.org/10.1002/2017JB014389.

Iannaccone, G., Guardato, S., Donnarumma, G.P., De Martino, P., Dolce, M., Macedonio, G., Chierici, F., Beranzoli, L., 2018. Measurement of seafloor deformation in the marine sector of the Campi Flegrei caldera (Italy). J. Geophys. Res. Solid Earth 123, 66–83. https://doi.org/10.1002/2017JB014852.

Isaia, R., Marianelli, P., Sbrana, A., 2009. Caldera unrest prior to intense volcanism in Campi Flegrei (Italy) at 4.0 ka B.P.: implications for caldera dynamics and future eruptive scenarios. Geophys. Res. Lett. 36, L21303. https://doi.org/10.1029/2009GL040513.

Isaia, R., Vitale, S., Di Giuseppe, M.G., Iannuzzi, E., Tramparulo, F.D.A., Troiano, A., 2015. Stratigraphy, structure, and volcano-tectonic evolution of Solfatara maar-diatreme (Campi Flegrei, Italy). Bull. Geol. Soc. Am. 127 (9–10), 1485–1504. https://doi.org/10.1130/B31183.1.

Kilburn, C., De Natale, G., Carlino, S., 2017. Progressive approach to eruption at Campi Flegrei caldera in southern Italy. Nat. Commun. https://doi.org/10.1038/ncomms15312.

Lee, S., Wolberg, G., Shin, S.Y., 1997. Scattered data interpolation with multilevel B-splines. IEEE Trans. Vis. Comput. Graph. 3 (3), 229–244.

Mayer, K., Scheu, B., Montanaro, C., Yilmaz, T.I., Isaia, R., Aßbichler, D., Dingwell, D.B., 2016. Hydrothermal alteration of surficial rocks at Solfatara (Campi Flegrei): petrophysical properties and implications for phreatic eruption processes. J. Volcanol. Geotherm. Res. 320, 128–143. https://doi.org/10.1016/j.jvolgeores.2016.04.020.

Moretti, R., De Natale, G., Troise, C., 2017. A geochemical and geophysical reappraisal to the significance of the recent unrest at Campi Flegrei caldera (Southern Italy). Geochem. Geophys. Geosyst. 1–18. https://doi.org/10.1002/2014GC005514.

Pedone, M., Aiuppa, A., Giudice, G., Grassa, F., Cardellini, C., Chiodini, G., Valenza, M., 2014. Volcanic CO2 flux measurement at Campi Flegrei by tunable diode laser absorption spectroscopy. Bull. Volcanol. 76 (4), 1–13. https://doi.org/10.1007/s00445-014-0812-z.

Queißer, M., Granieri, D., Burton, M., Arzilli, F., Avino, R., Carandente, A., 2017. Increasing CO2 flux at Pisciarelli, Campi Flegrei, Italy. Solid Earth 8 (5), 1017–1024. https://doi.org/10.5194/se-8-1017-2017.

R Core Team, 2013. R: A Language and Environment for Statistical Computing. R Foundation for Statistical Computing, Vienna, Austria, In: http://www.R-project.org/.

Venturi, S., Tassi, F., Cabassi, J., Vaselli, O., Minardi, I., Neri, S., … Virgili, G., 2019. A multi-instrumental geochemical approach to assess the environmental impact of CO_2-rich gas emissions in a densely populated area: the case of Cava dei Selci (Latium, Italy). Appl. Geochem. 101 (March 2018), 109–126. https://doi.org/10.1016/j.apgeochem.2019.01.003.

Verbesselt, J., Hyndman, R., Newnham, G., Culvenor, D., 2010. Detecting trend and seasonal changes in satellite image time series. Remote Sens. Environ. 114 (1), 106–115. https://doi.org/10.1016/j.rse.2009.08.014.

Verbesselt, J., Hyndman, R., Zeileis, A., Culvenor, D., 2010. Phenological change detection while accounting for abrupt and gradual trends in satellite image time series. Remote Sens. Environ. 114 (12), 2970–2980. https://doi.org/10.1016/j.rse.2010.08.003.

Zaccarelli, L., Bianco, F., 2017. Noise-based seismic monitoring of the Campi Flegrei caldera. Geophys. Res. Lett. 44, l. https://doi.org/10.1002/2016GL072477l.